ANALYSIS OF THE DYNAMIC BEHAVIOR OF CAPSULE ROBOT WHEN CHANGING THE IMPACT GAP OF THE VIBRATOR

Vu Van Dam[1], Nguyen Van Toan[2], Nguyen Van Du[3], Ngo Quoc Huy[3*]
[1]*TNU - University of Information and Communication Technology*
[2]*Military Institute of Mechanical Engineering,* [3]*TNU - University of Technology*

ARTICLE INFO

Received: **07/3/2025**
Revised: **12/4/2025**
Published: **12/4/2025**

KEYWORDS

Capsule robot
Dynamics response
Self-moving
Vibro-impact
Endoscopic capsule

ABSTRACT

The impact gap is an important structural parameter of the vibrator in a self-moving capsule device. This parameter needs to be set before packing the capsule robot. This study presents numerical simulation results evaluating the influence of impact gap on the dynamic behavior of the capsubot. Analytical techniques of time history plot, progression map, phase diagram, Poincaré map and bifurcation diagram are used to evaluate the system stability. The analysis results help designers have a technical basis to choose the appropriate impact gap in accordance with the operational requirements of the capsule. These results can be used to optimize control variables and design parameters, as a premise in building an experimental system to verify and evaluate the dynamic behavior of the capsubot system. This approach will also help reduce time and save costs on designing and manufacturing experimental models when developing active - controllable capsules.

PHÂN TÍCH ỨNG XỬ ĐỘNG LỰC HỌC ROBOT DẠNG VIÊN NANG KHI THAY ĐỔI KHOẢNG CÁCH VA ĐẬP CỦA BỘ TẠO RUNG

Vũ Văn Đam[1], Nguyễn Văn Toản[2], Nguyễn Văn Dự[3], Ngô Quốc Huy[3*]
[1]*Trường Đại học Công nghệ thông tin và Truyền thông - ĐH Thái Nguyên*
[2]*Viện Kỹ thuật cơ giới quân sự,* [3]*Trường Đại học Kỹ thuật Công nghiệp - ĐH Thái Nguyên*

THÔNG TIN BÀI BÁO

Ngày nhận bài: **07/3/2025**
Ngày hoàn thiện: **12/4/2025**
Ngày đăng: **12/4/2025**

TỪ KHÓA

Robot dạng viên nang
Ứng xử động lực học
Tự dịch chuyển
Rung-va đập
Viên nang nội soi

TÓM TẮT

Khoảng cách va đập là thông số kết cấu quan trọng của bộ tạo rung trong thiết bị tự di chuyển dạng viên nang. Thông số này cần được thiết lập trước khi đóng gói robot viên nang. Bài báo này trình bày các kết quả mô phỏng số đánh giá sự ảnh hưởng của khoảng cách khe hở va đập đến ứng xử động lực học của capsubot. Các kỹ thuật phân tích về đồ thị thời gian, bản đồ tiến trình, đồ thị pha, bản đồ Poincaré và đồ thị rẽ nhánh được sử dụng để đánh giá tính ổn định của hệ thống. Kết quả phân tích giúp người thiết kế có căn cứ kỹ thuật để lựa chọn khoảng cách khe hở va đập phù hợp với yêu cầu hoạt động của viên nang. Các kết quả này có thể được sử dụng để tối ưu hóa các biến điều khiển và tham số thiết kế, làm tiền đề xây dựng hệ thống thực nghiệm nhằm kiểm chứng và đánh giá ứng xử động học của hệ thống capubot thực. Cách tiếp cận này cũng sẽ giúp giảm thời gian và tiết kiệm chi phí thiết kế, chế tạo mô hình thử nghiệm khi phát triển viên nang chủ động, điều khiển được.

DOI: https://doi.org/10.34238/tnu-jst.12234

[*] Corresponding author. *Email: ngoquochuy24@tnut.edu.vn*

1. Introduction

Recently, self-moving capsule devices have been developed for endoscopic applications, diagnosis and treatment of gastrointestinal diseases [1] - [3]. This is a research direction that helps turn passive endoscopic capsules into capsules that can move on their own according to external control signals, helping to increase the ability to reach the correct damaged area to observe and treat gastrointestinal diseases. The mini robots using legs, padding, inchworm-like mechanism, spiral wing motor, suction cup principle [3], are difficult to enclose in a smooth capsule shape. Moving parts can damage the walls of the digestive tract. The solutions of using an external magnetic field to forcefully control the capsubot have also been tested by many research groups, as shown in the review by Chen et al. [4]. This method essentially exploits the magnetic interaction between an external magnetic field source acting on a permanent magnet inside the capsule model. In this way, capsubot can move to accurately access the area that needs to be observed for diagnosis, sampling or treatment safely and non-invasively. To control external magnetic fields, handheld devices [5], robotic arms [6], [7] or specialized rotating magnetic field creation systems [8], [9] can be used. The biggest advantage of this method is that the capsule is small in size, light in weight, and generates low temperature. However, a significant challenge arises in maintaining the equilibrium of the magnetic force exerted by the external permanent magnet on the capsule robot. When this force becomes unbalanced, the capsule may become immobilized. Increased friction between the capsule and the intestinal wall during movement can potentially result in damage to the intestinal tissue. Generally, solutions that utilize external magnetic fields for navigating capsule endoscopy present several disadvantages. These include the risk of causing harm to the patient's body due to the effects of a strong magnetic field, the dependence of magnetic force on both distance and body thickness, as well as the complexity and high cost associated with the magnetic field control system.

The capsubot design direction that exploits the vibration-impact effect using vibrators located inside the capsule is considered a viable alternative. This principle exploits the sudden change in inertial force arising upon impact (vibro-impact), to overcome resistance from the environment, thereby creating displacement of the mechanical system [10], [11]. By this way, the device can be enclosed in a smooth capsule, also known as capsule robot or capsubot. The basic physical model describing the vibro-impact capsule robot system is described in Figure 1, in which, the inertial mass m_1, excited by the electromagnetic force F_m, moves back-forth and impacts the capsubot body m_2. A linear spring k and a viscous damper c is used to connect the two masses m_1 and m_2. The friction force between m_1 and m_2 is assumed to be zero. X_1 and X_2 represent the absolute displacements of the two masses, respectively. In the initial position, when m_1 is not excited, the distance between m_1 and m_2 is denoted by G. The internal mass m_1 will impact to the capsubot body when the relative displacement X_1-X_2 is greater than or equal to the gap G value. The impact stiffness between the two masses m_1 and m_2 is characterized by a linear spring with stiffness k_0.

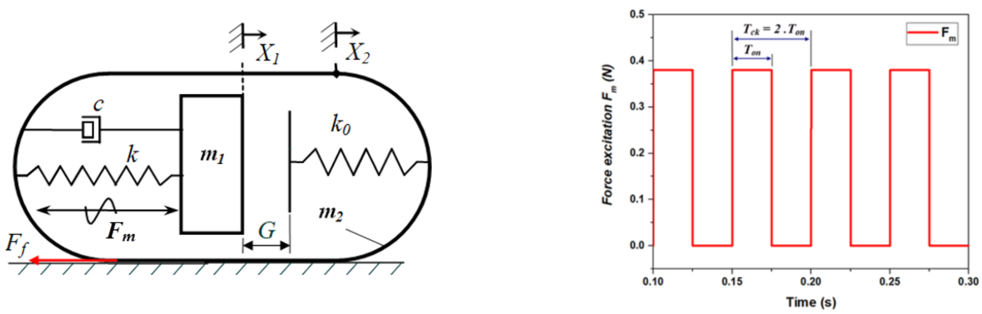

(a) (b)

Figure 1. *(a) Basic physical model of vibro-impact capsule robots, (b) The excitation force F_m with the square wave signal*

Up to now, the basic principle commonly applied to the vibrator has been to use the electric-magnetic force interaction to create linear motion of the mass m_1. Experimental models for capsubots using this principle have been proposed by many research groups, such as solenoids [12] - [14], eccentric motors [15], round-trip pendulums [16], electromechanical vibrators [17] or linear motors [18]. However, these devices are still quite large and cumbersome, requiring physical wires to transmit energy and control signals, potentially hindering movement and damaging the digestive tract wall. Although the large size of the device is convenient for installing measuring devices to support the experimental process. It is an obstacle and difficult to develop for small-sized capsubot applications.

Design requirement of the capsubot is able to self-moving under external control signals. It is necessary to eliminate physical wires and be packaged in a capsule shell as shown in Figure 1. Therefore, a vibrator, a power source, and a device to receive control signals from the outside need to be arranged inside the capsule. The main difficulty is the limitation of the space size inside the small capsule and the working equipment modules. In particular, when installing the vibrator, it is necessary to set a reasonable and fixed impact gap in advance. When the capsule is closed, it will be difficult to change this size. Studies also show that impact gap as a great influence on the robot's ability to operate [19], [20]. To choose this structural parameter properly, it is necessary to calculate and realistically evaluate the displacement ability of the capsule. This study presents results using numerical simulation solutions to evaluate the influence of impact gap on the dynamic behavior of the capsubot. This method will help determine a reasonable G, reduce calculation time, the number of changes to the vibrator structure. The numerical simulation results will also serve as a premise for building experimental models and developing applications of capsubot.

2. Materials and Methods

Modelling of vibro-impact capsubot is proposed, including: *mathematical model, and wireless control capsubot model.*

2.1. Mathematical model

The mathematical model describing the motion of the capsubot (Figure 1) can be expressed as follows:

$$\begin{cases} m_1 \ddot{X}_1 = F_m - k.X_{rel} - c.V_{rel} - H.F_{imp} \\ m_2 \ddot{X}_2 = -F_m + k.X_{rel} c.V_{rel} + H.F_{imp} - F_f \end{cases} \quad (1)$$

Where, the relative displacement and relative velocity between the masses m_1 and m_2 are defined as $X_{rel} = X_1 - X_2$ and $V_{rel} = \dot{X}_1 - \dot{X}_2 = (dX_1/dt - dX_2/dt)$, respectively.

The impact force F_{imp} between m_1 and m_2 is represented as follows:

$$F_{imp} = k_0(X_1 - X_2 - G) \quad (2)$$

The Heaviside function H describes the impact interaction between m_1 and m_2 as follows:

$$H = \begin{cases} 1, & \text{if } (X_1 - X_2 - G) > 0 \\ 0, & \text{if } (X_1 - X_2 - G) \le 0 \end{cases} \quad (3)$$

The friction force component F_f is represented in the form of Coulomb friction:

$$F_f = (\mathrm{m_1}+\mathrm{m_2}).\mathrm{g}.\mu.\mathrm{sign}\left(\dot{X}_2\right) \quad (4)$$

In which, g is the gravitational acceleration; μ is the Coulomb coefficient of friction between the capsubot and the environment. The "*sign"* function represents the direction of the frictional force, which opposes the direction of motion.

The excitation force, $F_{m,}$ depends on the excitation square signal form, frequency *f,* and current, as illustrated in the following equation:

$$F_m = F_0 .heav(\sin(2\pi ft)) \quad (5)$$

Where: F_0 is the excitation force amplitude, f is the excitation frequency and t is time. F_0 depends on the coefficient, *BL* and the current amplitude, i_0, expressed by the equation $F_0 = (B.L).i_0$. The excitation force F_m with the square wave signal, $i_0 = 0.5$ A, $f = 20$ Hz is shown as Figure 1b.

2.2. Wireless control capsubot model

A model of a self-moving capsule device using a battery combined with a Bluetooth signal receiver is proposed as shown in Figure 2. The commercial Linear Voice Coil Motor (LVCM-013-032-02) is used as the vibrator for the capsubot, with the characteristic coefficient of the electromagnetic interaction force between the wire tube and the permanent magnet core given by B*L= 0.76N/A. A lithium-ion battery (LIR1654 -120 mAh) is used as the power source for both the DW-CT14 amplifier circuit and the oscillation motor. The excitation signal is provided by a function generator, which transmits the signal to the amplifier circuit via a Bluetooth USB receiving antenna. When an oscillating electrical signal form square-pulse is amplified for the coil of the vibrating motor, it causes the magnet core m_1 to oscillate and impact the stopper. The inertial force of the moving mass m_1, combined with the impact force and spring elastic force, creates an interaction between the capsule shell and the environment, causing the capsubot to move. To create the interaction between m_1 and m_2, a linear conical spring is used in the inner tube of coil with stiffness *k* and damping coefficient *c*. The displacement of the capsubot is measured by the Micro Laser Distance Sensor (HG-C1100). The measured signal is recorded by the DAQ NI USB-6008 and stored on a computer using NI SignalExpress software. The structural and control parameters for the proposed capsule model are selected as shown in Table 1.

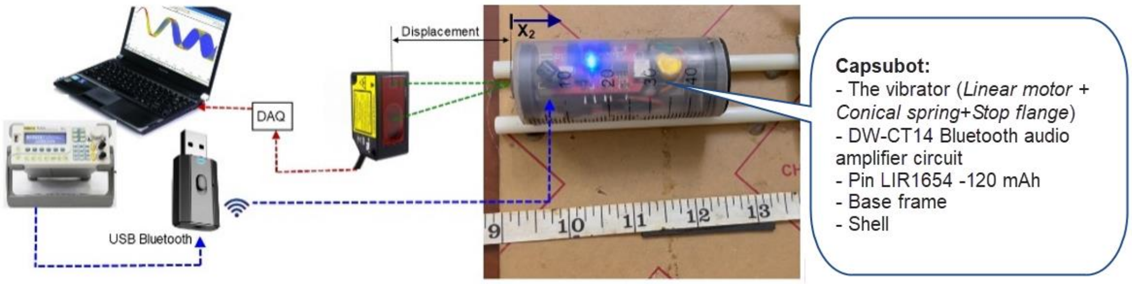

Figure 2. *Wireless control capsubot system*

Table 1. *Experimental parameters of the proposed capsubot model*

Parameter	Notation	Value	Unit
Internal mass	m_1	0.007	Kg
Body mass	m_2	0.043	Kg
Coefficient LVCM (Force constant)	BL	0.76	N/A
Impact gap	G	0 - 3	mm
Coefficient of friction	μ	0.275	-
Stiffness of spring	k	178.19502	N/m
Stiffness of impact	k_0	980000	N/m
Damping coefficient	c	0.1736	Ns/m
Excitation current	i_0	0.2–0.8	A
Excitation frequency	f	10–40	Hz
Dimension	R x Lc	0.015x0.07	m

Next, numerical simulation method is used to investigate and evaluate the mathematical model of the proposed capsubot. Equation (1) has strong nonlinear characteristics, containing many influencing parameters, especially the function describing the state of impact (Equation (3)). XPPAuto software is used to find solutions for Equation (1). The solution program is written in code form, convenient for changing the initial condition parameters. The resulting data are analyzed, evaluated and presented through the Originlab tool. In this way, the values of the impact gap *G* will be investigated at the different excitation force and frequencies levels. Analytical techniques of time history plot, the progression map, the phase diagram – Poincaré map, the bifurcation diagram will be used to evaluate the dynamic behavior of the capsubot when changing the impact gap *G*.

3. Results and Discussion

3.1. Effect of the impact gap G and frequency f to the obtained progression

With a battery-powered capsule system (Figure 2), the battery capacity will decrease over time because it has to supply both the amplifier circuit and the vibrator. This means that the current supplied to the coil of the vibrator will also decrease over time. Through calculation, three levels of excitation current i_0 = 0.2, 0.5 and 0.8A will be investigated. To evaluate the achieved displacement progression of capsubot after the same time period 5 seconds, the scanning function to simultaneously survey both parameters of excitation frequency *f* and impact gap *G* on XPPAuto software will be exploited. The investigation results are shown in Figure 3.

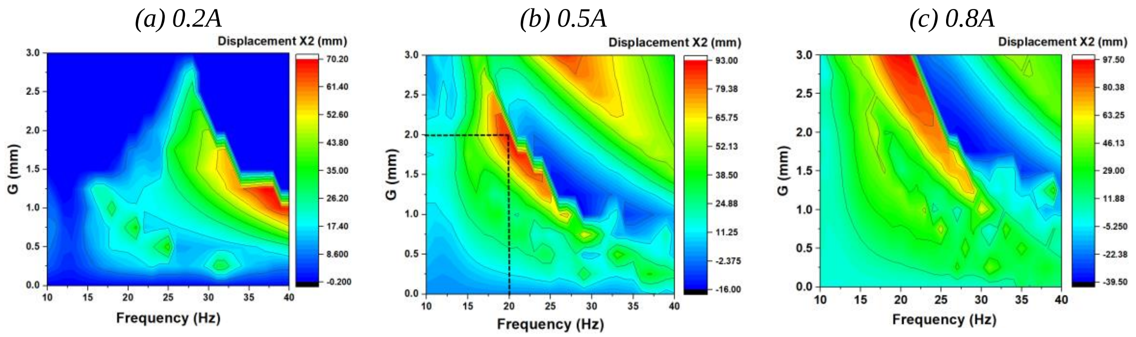

Figure 3. *Displacement after 5s of the capsubot when changing impact distance G and frequency f at three excitation force levels*

In Figure 3a, at the value of excitation force corresponding to the current amplitude supplied to the vibrator i_0 = 0.2 A, the capsubot almost only moves forward and the objected backward progression of capsubot is very small (*-0.2 mm, the blue region*). With the impact gap area, *G* = [1-1.25] mm, the forward displacement of the capsubot increases as the excitation frequency increases, and reaches the largest forward value when *f* = 35-40 Hz (*the red region)*. However, with the requirement to be controllable, the capsubot needs to be able to move forward and backward to the specified positions. When capsubot is working, the excitation frequency and the current supplied to the vibrator are often chosen as control parameters. These two parameters are set by the function generator and wirelessly transmitted to the amplifier circuit via USB Bluetooth, as depicted in Figure 2. Besides the criterion of the objected progression, choosing the impact gap *G* needs to consider the ability to control the direction of the capsubot forward and backward by changing the frequency and excitation current. Figure 3b depicts the progression map of the capsubot after 5s when changing the frequency and impact gap with the amplytude of excitation current i_0 = 0.5 A. In the range of gap *G* = (1-2) mm, the capsubot can move forward and backward when changing the frequency of the excitation signal. The red region in Figure 3b shows the largest objected progression after 5s corresponding to the values of *G* and *f*. With the investigated parameter ranges, the average speed of backward moving after 5s was quite slow compared to forward moving (3.2 mm/s compared to 18.6 mm/s). At a large excitation force amplitude level, i_0 = 0.8 A, the gap G can be selected in the range of (1.5-3) mm to achieve the requirement of controlling the direction of motion by changing the excitation frequency. The desired forward and backward progression can be completely controlled by selecting the impact gap corresponding to the excitation frequency. However, when the capsubot operates with a large excitation current i_0, the battery capacity will decrease rapidly, the operating time of the capsubot will be short, causing heat generation. Depending on the control purpose, if the capsubot wants to achieve fast movement speed then the parameters (G, f) are selected and set according to the graph Figure 3a. On the contrary, if the capsubot wants to achieve a long operating time, then the control parameters (G, f) should be selected according to the relationship shown in Figure 3a. To achieve effective operating time and movement speed, the current i_0 = 0.5 A is selected to continue analyzing and evaluating the level of dynamic stability for the capsubot. Figure 4 shows more clearly the analysis results of the objected progression after 5s, for the point (G = 2 mm, f = 20 Hz) marked on Figure 3b.

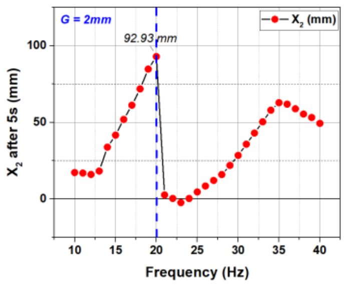

(a)

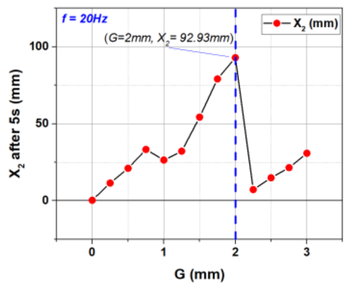

(b)

Figure 4. *The objected progression after 5s when the frequency changes with G = 2 mm (a) and the impact gap G changes with f = 20Hz,* i_0 *= 0.5 (b)*

3.2. The time history plot and progression map, y_P

Capsubot is investigated the displacement progression when setting G = 2mm, f = 20 Hz and i_0 = 0.5 A. This is very important to evaluate the interaction between its dynamic response and the obtained progression. Figure 5 shows the results of analyzing the displacement progression X_2 of the capsubot over time. In particular, Figure 5a is a time history plot, showing the displacement of the capsubot with the relative displacement $X_{rel} = X_1\text{-}X_2$ of m_1 and m_2.

At the moment of impact, the displacement progression exhibits a sudden variation (or jump), resulting in the relative displacement being fixed at the position of the stop-impact flange. The '*progression per period*' values, denoted as y_P, are calculated as the difference between X_2 at the end and X_2 at the beginning of each excitation period, T_P, across two adjacent slices. y_P is shortly called "progression map". This is a map describing the set of points y_P over time t. Using the OriginLab data analysis tool, the "Reduce to Evenly Spaced X" function is employed to evenly distribute data points along the time axis within the dataset. This function facilitates the determination of the variation of the progression per period y_P over time. The progression map is presented in Figure 5b. Furthermore, the stability of the capsule robot's movement is directly correlated with the proximity of the y_P points. Specifically, when the y_P points are closer together or distributed within a narrower range, this indicates reduced fluctuations. Consequently, such a reduction in variability contributes to a more stable movement of the capsule robot.

The time history plot visually illustrates the trends in system behavior as survey parameters are altered. By the time history plot and the progression map, we can roughly evaluate the dynamic characteristics of the system. However, very little other information can be found using this analysis technique and be difficult to analyze and evaluate the dynamic characteristics and behavior of the system. To solve this problem, phase diagram, Poincare' map and bifurcation diagram analysis techniques are used.

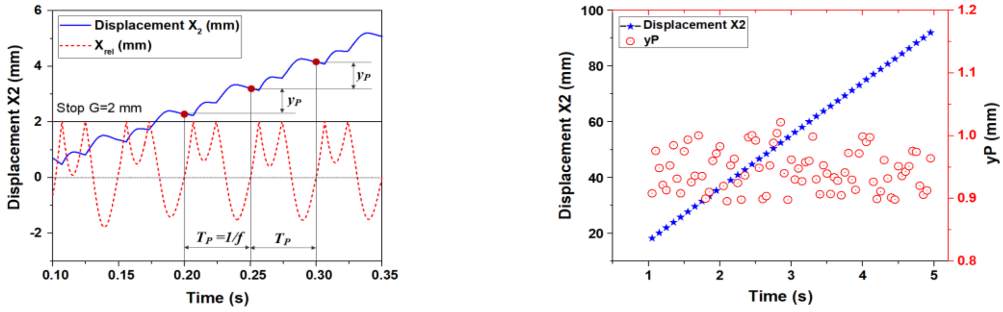

(a) *(b)*

Figure 5. *(a) Time history plot showing the displacement process X_2 , X_{rel} and (b) the progression map or variation of y_P over time. The excitation of f = 20Hz, i_0 = 0.5A was applied when setting G=2mm*

3.3. Phase diagrams and Pointcaré map

The phase diagram is often represented through the relationship between the relative displacement X_{rel} and the relative velocity V_{rel} of two masses m_1 and m_2. Due to the elimination of the time axis, the phase diagram allows many motion cycles to be superimposed on each other in a small representation space. Thanks to the phase diagram, it is possible to see whether the capsubot's motion rules are stable between working cycles or not. Figure 6a shows the phase trajectories of 100 cycles of excitation force and the Pointcaré map. The Pointcaré slice technique is used to contruct the Pointcaré map. At the moment when the excitation force decreases to F_m= 0, the coordinates of the point (X_{rel-P} - V_{rel-P}) are recorded on the phase trajectory over one excitation cycle period, as illustrated in Figure 6.b. The Poincaré points, marked in red, are positioned along the phase trajectory lines across 100 survey cycles, exhibiting a discrete distribution that forms a dense region of red dots without overlap (as depicted in the enlarged image in the center of Figure 6a), thereby creating the Poincaré map. Therefore, the analysis of the phase map indicates that the motion of the proposed capsule exhibits characteristics of unstable and chaotic behavior. Additionally, Figure 6.b illustrates the phase trajectory over one excitation cycle, highlighting two impacts between between m_1 and m_2 that occur during each cycle. This observation is consistent with the time history plot presented in Figure 5a.

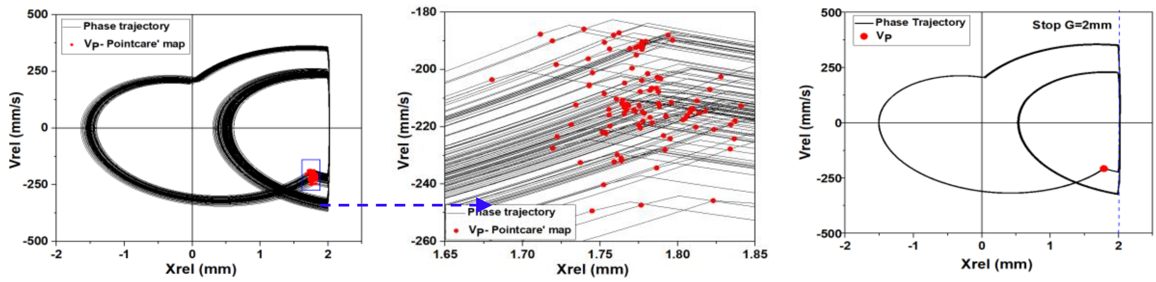

(a) (b)

Figure 6. *The phase diagram and Pointcaré map of capsubot (a) with 100 cycles and (b) with one excitation period*

3.4. Bifurcation diagram

Bifurcation analysis was applied to examine the stability of the system. The bifurcation diagram represents the relationship between the relative velocities and the excitation frequency ($V_{rel} - f$). At a excitation frequency value, the values of the relative velocity V_{rel} are determined. The special value of frequency that causes a sudden variation of V_{rel} that reflects the behavioral characteristics of the system is called the bifurcation value. The bifurcation value refers to the excitation signal frequency f at which the relative velocity V_{rel} between masses m_1 and m_2 begins to bifurcate into two distinct curves. After biffurcating, at the next excitation frequency two states will occur. At some excitation cycles, the relative velocity will be distributed over a branch. At some other period, the relative velocity falls into the other branch. When the control variable (f) changes, the obtained relative velocity values V_{rel} will create a bifurcation diagram. In this study, it is built by using numerical simulation method with XPPauto software. Figure 7 shows the relative velocity V_{rel} corresponding to the surveyed frequency value. This is also the bifurcation diagram that reflects the stability of the capsubot under survey conditions. In the range of frequency f = (10.6 - 11.4) Hz, capsubot works in a state of chaotic motion. At most other excitation frequencies, there are strong fluctuations in the relative velocity V_{rel}, indicating that the capsubot moves unstable. At the high excitation frequencie range (27 - 40) Hz, the relative velocity variation will be wider. Especially at the frequency of 20.6 Hz, there is a sudden jump from forward to backward motion, sensitive to changes in the excitation frequency signal, leading to difficulty in control at this excitation frequency range. These are the results of dynamic analysis in a typical case with the condition of impact gap G = 2 mm and excitation current i_0 = 0.5 A. In other working conditions, the implementation method to evaluate the dynamic behavior of the capsubot will be similar. Under the initial excitation conditions investigated, the results show that the motion has no the biffurcation and the bifurcation value (point) is undetermined.

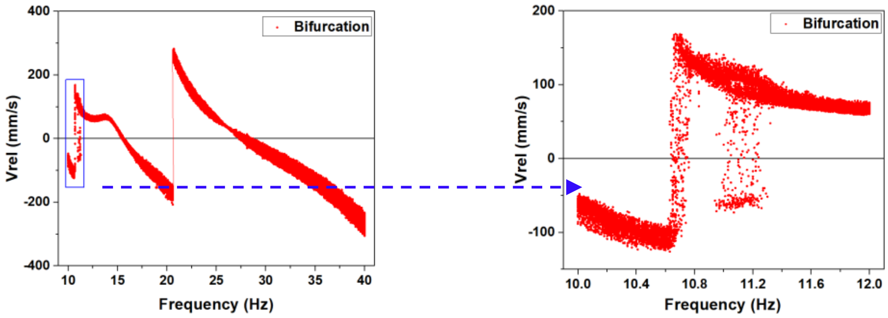

Firure 7. *The bifurcation diagram of the relative velocity, V_{rel}, with respect to various excitation frequency, f*

4. Conclusion

This study presents the results of analyzing the influence of impact gap on the dynamic behavior of the capsubot. The interactive influence between structural parameters (*the impact gap G*) and control parameters *(frequency f and excitation current i_0*) are evaluated. Five techniques are used to analyze the dynamic behavior of the capsubot, including: the time history plot, the progression map, the phase diagram, Poincaré map and the bifurcation diagram.

These numerical investigation results will help the designer choose the structural parameter, G, and arrange the impact flange for the vibrator appropriately, before putting it into the sealed capsule. To achieve good displacement, aiming to save energy and prolong battery working time, the impact distance should be chosen G = 2 mm. Based on control requirements, the capsubot can be set up by selecting the parameters (G, f, i_0). The results will help to optimize control variables and design parameters and to reduce time and costs in designing and manufacturing experimental models for developing active capsules. With the operating principle of an internal battery-powered vibrator using this Bluetooth control signal, the capsubot can be developed and tested in many environments close to real working conditions, in addition to dry friction conditions.

The numerical solution is very meaningful in investigating and selecting optimal parameters. However, the use of the Culomb friction model is still different from the actual working conditions aimed at the capsule in the gastrointestinal tract containing fluid and mucosal folds. Experimental results investigating of capsule navigational capabilities; evaluating of dynamic stability; verifying the suitability of the model as well as the actual dynamic behavior of the capsule robot in different environments will be published in upcoming studies.

Acknowledgments

This research was funded by the Thai Nguyen University of Technology (TNUT), Code number of project T2024-NCS01.

REFERENCES

[1] M. D. Vasilakakis *et al.*, "The future of capsule endoscopy in clinical practice: from diagnostic to therapeutic experimental prototype capsules," *Prz Gastroenterol*, vol. 15, no. 3, pp. 179-193, 2020.

[2] I. Hossain, R. Alam, and K. A. A. Mamun, "A Review of Locomotion Mechanism for Wireless Capsule Endoscopy," *International Journal of Innovative Research in Electrical, Electronics, Instrumentation and Control Engineering,* vol. 7, no.7, pp. 46 - 53, 2019.

[3] L. Liu, S. Towfighian, and A. Hila, "A Review of Locomotion Systems for Capsule Endoscopy," *IEEE Rev Biomed Eng*, vol. 8, pp. 138-151, 2015.

[4] W. Chen, J. Sui, and C. Wang, "Magnetically Actuated Capsule Robots: A Review," *IEEE Access,* vol. 10, pp. 88398-88420, 2022.

[5] C. R. Simons-Linares and J. J. Vargo, "Use of Magnets in Flexible Endoscopy," in *Magnetic Surgery*, M. Gagner, Editor. Springer International Publishing, 2021, pp. 95-107.

[6] Y. Xu *et al.*, "Autonomous Magnetic Navigation Framework for Active Wireless Capsule Endoscopy Inspired by Conventional Colonoscopy Procedures," *IEEE Robotics and Automation Letters,* vol. 7, no. 2, pp. 1729-1736, 2022.

[7] K. Incetan *et al.*, "VR-Caps: A Virtual Environment for Capsule Endoscopy," *Med Image Anal*, vol. 70, 2021, Art. no. 101990.

[8] Z. Yang *et al.*, "Magnetically Actuated Continuum Medical Robots: A Review," *Advanced Intelligent Systems*, vol. 5, no. 6, 2023, doi: 10.1002/aisy.202200416 .

[9] H. Wang *et al.*, "Magnetic soft robots: Design, actuation, and function," *Journal of Alloys and Compounds,* vol. 922, 2022, Art. no. 166219.

[10] E. Pavlovskaia, M. Wiercigroch, and C. Grebogi, "Modeling of an impact system with a drift," *Phys. Rev. E. Stat. Nonlin. Soft Matter. Phys.*, vol. 64, no. 5, Pt. 2, 2001, Art. no. 056224.

[11] K. T. Nguyen *et al.*, "Stability of vibro-impact driven locomotion system with random initial conditions," *TNU Journal of Science and Technology*, vol. 226, no. 11, pp. 10-19, 2021.

[12] V.-D. Nguyen *et al.*, "A New Design of Horizontal Electro-Vibro-Impact Devices," *Journal of Computational and Nonlinear Dynamics*, vol. 12, no. 6, 2017, Art. no. 061002.

[13] K. A. Sapronov, A.A. Cherepanov, and S. F. Yatsun, "Investigation of motion of a mobile two-mass vibration-driven system," *Journal of Computer and Systems Sciences International,* vol. 49, no. 1, pp. 144-151, 2010.

[14] A. N. Grankin, and S. F. Yatsun, "Investigation of vibroimpact regimes of motion of a mobile microrobot with electromagnetic drive," *Journal of Computer and Systems Sciences International*, vol. 48, no. 1, pp. 155-163, 2009.

[15] R. Carta *et al.*, "A multi-coil inductive powering system for an endoscopic capsule with vibratory actuation," *Sensors and Actuators A: Physical,* vol. 172, no. 1, pp. 253-258, 2011.

[16] P. Liu *et al.*, "A self-propelled robotic system with a visco-elastic joint: dynamics and motion analysis," *Engineering With Computers,* vol. 36, pp. 655–669, 2019.

[17] V.-D. Nguyen and N.-T. La, "An improvement of vibration-driven locomotion module for capsule robots," *Mechanics Based Design of Structures and Machines*, vol.50, pp. 1658-1672, 2020.

[18] Y. Liu, E. Pavlovskaia, and M. Wiercigroch, "Experimental verification of the vibro-impact capsule model," *Nonlinear Dynamics*, vol. 83, no. 1-2, pp. 1029-1041, 2015.

[19] G. Stefani, M. D. Angelis, and U. Andreaus, "Influence of the gap size on the response of a single-degree-of-freedom vibro-impact system with two-sided constraints: Experimental tests and numerical modeling," *International Journal of Mechanical Sciences*, vol. 206, 2021, Art. no. 106617.

[20] Y. Liu *et al.*, "Bifurcation analysis of a vibro-impact experimental rig with two-sided constraint," *Meccanica*, vol. 55, pp. 2505–2521, 2020.